

Mathematics Notes
Note 74

November 1981

Detection of Branch Points by Modified FFT

Fung I. Tseng and Tapan K. Sarkar
Department of Electrical Engineering
Rochester Institute of Technology
Rochester, New York 14623

Abstract

This paper illustrates the existence of branch points in transients on lossy transmission lines and presents a technique of detecting branch points. By applying modified FFT to the transient signal and from the resulting amplitude and phase spectra, it is possible to detect and distinguish branch points from poles. Numerous examples are given to demonstrate the effectiveness of the modified FFT and the use of windowing in improving the detectability of a small branch point under the influence of a nearby strong pole.

1. INTRODUCTION:

In recent years significant interest has been focused on the problems of target identification and remote sensing. To determine the physical properties of a target one illuminates it with a wide-band signal and determines the singularities in the transient response. The target is usually modeled as a lumped-parameter system. The transfer function of the system is often assumed to consist of simple poles only. It was pointed out by Baum [1] that for a general target the response might contain singularities other than simple poles. Franceschetti [2]-[3] showed that, in a dispersive environment, the branch-out contribution plays a dominant role at large observation times. In the case of transients on a lossy transmission line it is well known that the branch points play an important role in the transient analysis [4]-[5]. Recently, Tai [6] applied singularity expansion methods to analyze the transients on a lossless line. In this paper we illustrate the existence of branch points in transient responses for two cascaded lossy transmission lines. The main purpose of this paper is to present a technique of detecting branch points. By applying a recently developed modified FFT to the transient signal, we are able to employ both the phase and the amplitude spectra to detect and distinguish branch points from poles. By proper application of windowing we also show the possibility of improving detectability of a small branch point under the influence of a nearby strong pole.

2. Branch Points in a Transient on a Lossy Transmission Line:

We consider two lines of lengths ℓ and d cascaded as shown in Figure 1. The lines connect an arbitrary generator $V_g(s)$ of impedance $Z_g(s)$ with an arbitrary load impedance $Z'_L(s)$. The lines are lossy and uniform but there is a discontinuity at $x=\ell$ (or $x'=0$) where the voltage is designated as $v_L(t)$, which has a Laplace Transform $V_L(s)$. Let T be the delay time from $x=0$ to $x=\ell$ and T' be the delay time from $x'=0$ to $x'=d$, then for $0 < t < t_1$ (t_1 is the smaller of T' or $3T$) the voltage $v_L(t)$ is given by [5].

$$v_L(t) = \mathcal{L}^{-1} [V_L(s)]$$

$$= \mathcal{L}^{-1} \left\{ 2V_g(s) \cdot \frac{Z_0(s)}{Z_0(s) + Z_g(s)} \cdot \frac{Z'_0(s)}{Z_0(s) + Z'_0(s)} \exp[-\ell\gamma(s)] \right\}$$

$$0 < t < t_1 \quad (1)$$

where \mathcal{L}^{-1} denotes the inverse Laplace transform. The characteristic impedance $Z_0(s)$ and propagation function $\gamma(s)$ of the transmission line ℓ are given by

$$Z_0(s) = [Z(s)/Y(s)]^{\frac{1}{2}} \quad (2)$$

$$\gamma(s) = [Z(s)Y(s)]^{\frac{1}{2}} \quad (3)$$

where the transmission-line series impedance/meter $Z(s)$ and shunt admittance/meter $Y(s)$ are given by [5] for a coaxial cable:

$$Z(s) = sL + A_0 s^{\frac{1}{2}} + \sum_{k=0}^2 A_{k+1} s^{-k/2} + \phi s^{-2} \quad (4)$$

$$Y(s) = sC \quad (5)$$

Eq. (4) is for high frequency approximation. ϕ is a function of the conductor physical dimensions and material parameters. The coefficient A_0 represents planar skin effect while A_1 through A_3 introduce cylindrical lower-frequency corrections. The coefficients are functions of the radii of the coaxial cable and are given in [5]. Here what we are interested in is the fact that both $Z(s)$ and $Y(s)$ are functions of complex frequency $s = \sigma + j\omega$ even for high-frequency approximation. In (1) Z_0' is the characteristic impedance of line d, which has similar expressions as given by Eqs. (2) through (5):

$$Z_0'(s) = [Z'(s)/Y'(s)]^{\frac{1}{2}} \quad (6)$$

$$Y'(s) = [Z'(s)Y'(s)]^{\frac{1}{2}} \quad (7)$$

where

$$Z'(s) = sL' + A_0'(s)^{\frac{1}{2}} + \sum_{k=0}^2 A'_{k+1} s^{-k/2} + \phi' s^{-2} \quad (8)$$

$$Y'(s) = sC' \quad (9)$$

From (2), (4), (6) and (8) it can be seen that the branch points of $v_L(t)$ are given by the roots of

$$sL + A_0 s^{\frac{1}{2}} + \sum_{k=0}^2 A_{k+1} s^{-k/2} + \phi s^{-2} = 0 \quad (10)$$

$$sL' + A_0' s^{\frac{1}{2}} + \sum_{k=0}^2 A'_{k+1} s^{-k/2} + \phi' s^{-2} = 0 \quad (11)$$

Since the coefficients ϕ , ϕ' , A_k and A'_k ($k=0$ to 3) are functions of the physical dimensions and material parameters of the transmission lines, the branch points of $v_L(t)$ are also functions of these parameters. Now part of $v_L(t)$ will be reflected back to the source, thus the received signal at the source will contain poles and branch points which characterize both transmission lines.

3. Detection of Branch Points by Modified FFT:

(a) Modified FFT.

It was shown in [7] that one can modify FFT to evaluate the z-transform of a time sequence along a general contour on the complex frequency plane. The modified FFT then plays the role in a discrete system which is played by the Laplace transform in a continuous system.

Assume the time response $x(t)$ is uniformly sampled at a sampling rate of f_s Hz. Let $T = 1/f_s$ be the sampling time interval. Let $\{s_k\}$ be the complex frequency along the straight line $s = -\sigma_0$, then $s_k = -\sigma_0 + j\omega_k$, where $\omega_k = 2\pi k f_s / N$. The Laplace transform of $x(t)$ can then be evaluated by

$$X(s_k) = \sum_{n=0}^{N-1} (x_n e^{+\sigma_0 nT}) e^{-j2\pi nk/N} \quad (12)$$

Eq. (12) shows that to evaluate $X(s)$ along a straight line $s = -\sigma_0$ on the complex plane, one can multiply the sequence $x_n = x(nT)$ by $\{e^{\sigma_0 nT}\}$ and then take the FFT.

(b) Phase Variation near the Singularities.

Consider a received signal $x(t)$ with a Laplace transform $X(s)$. Assume there are N pairs of simple poles $s_{pn} = -\alpha_n \pm j\beta_n$, $n=1,2,\dots,N$, and M pairs of branch points $s_{bm} = -\sigma_m \pm j\delta_m$, $m=1,2,\dots,M$. We write the $X(s)$ as:

$$X(s) = \sum_{n=1}^N a_n \left(\frac{1}{s-s_{pn}} + \frac{1}{s-s_{pn}^*} \right) + \sum_{m=1}^M b_m \left(\frac{1}{(s-s_{bm})(s-s_{bm}^*)} \right) \quad (13)$$

Taking inverse Laplace transform of (13) yields

$$x(t) = 2 \sum_{n=1}^N a_n e^{-\alpha_n t} \cos \beta_n t + \sum_{m=1}^M b_m e^{-\sigma_m t} J_0(\delta_m t) \quad (14)$$

where $J_0(t)$ is the zero-th order Bessel function. Notice that we have implicitly assumed that $\{a_n\}$ and $\{b_m\}$ are real numbers for simplicity. Now if the modified FFT is evaluated along the contour $\sigma = -\sigma_0$ which is very close to a pole at s_{pn} as shown in Figure 2, then at A and B we have

$$X(s_A) \approx \frac{a_n}{s_A - s_{pn}} = \frac{a_n e^{j\theta_A}}{|\epsilon_A|} \quad (15)$$

and

$$X(s_B) \approx \frac{a_n}{s_B - s_{pn}} = \frac{a_n e^{-j\theta_B}}{|\epsilon_B|} \quad (16)$$

The phase variation is $(\theta_A + \theta_B)$. If the contour is very close to the pole s_{pn} then $(\theta_A + \theta_B)$ will approach 180° .

If the contour is passing by a branch point s_{bm} then

$$X(s_A) \approx \frac{b_n}{(s_A - s_{bm})(s_{bm} - s_{bm}^*)} = \frac{b_n \exp(j\frac{1}{2}\theta_A)}{\epsilon_A (s_{bm} - s_{bm}^*)} \quad (17)$$

and

$$X(s_B) \approx \frac{b_n}{(s_B - s_{bm})(s_{bm} - s_{bm}^*)} = \frac{b_n \exp(-j\frac{1}{2}\theta_B)}{\epsilon_B (s_{bm} - s_{bm}^*)} \quad (18)$$

The phase variation is now $\frac{1}{2}(\theta_A + \theta_B)$, which approaches 90° if the contour is very close to the branch point. The above analysis shows that we could detect a singularity by observing a large variation of phase angle of the modified FFT. We can also distinguish a branch point from a pole by observing whether the phase variation is close to 90° or 180° .

Fig. 1

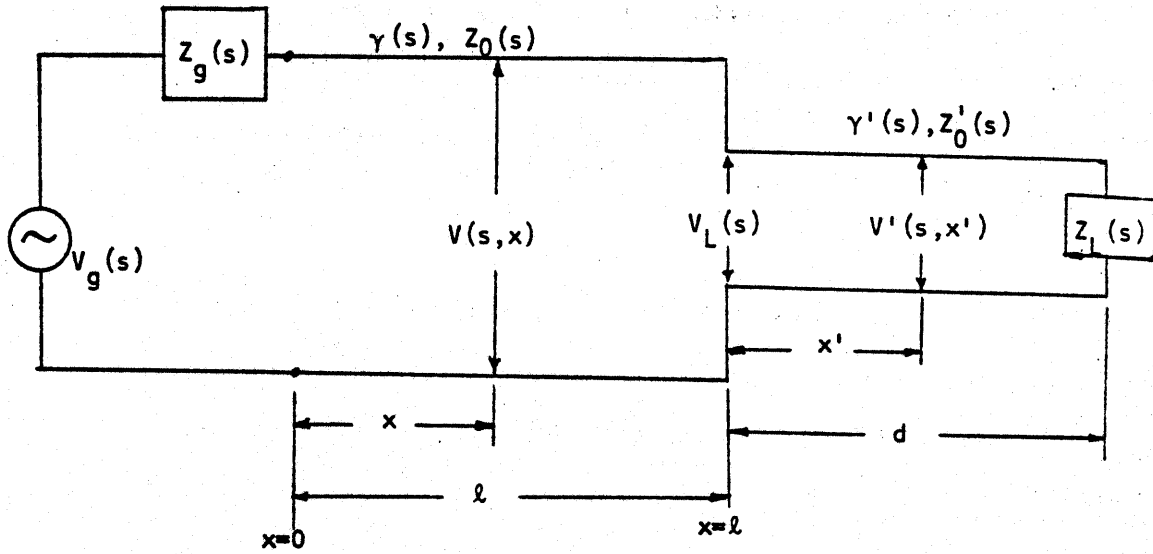


Fig. 1. Cascaded Lossy Transmission Lines

Fig. 2

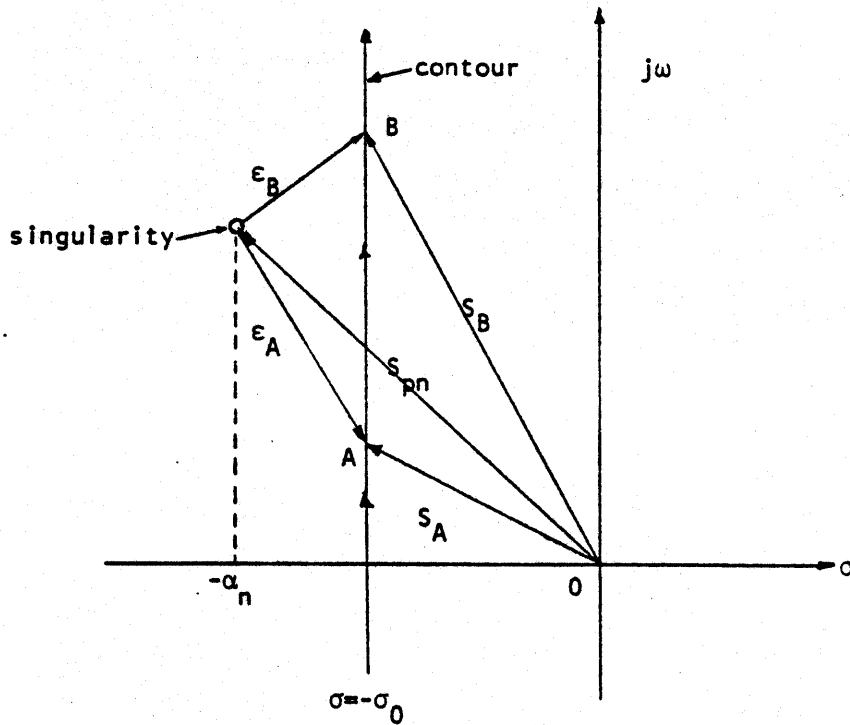


Fig. 2. Detection of branch points and poles by phase variations.

(c) Windowing to Improve Detectability.

Since the data sequence is finite, the modified FFT suffer from leakage effects, which results in high near-sidelobes in the spectral window. Thus to improve the detection of a small singularity (branch point or pole) in the presence of a nearby strong singularity we shall apply a special Tseng window [8] designed to have low near-sidelobes to the modified FFT.

The detailed Tseng window design technique has been presented in [8]. Here we outline the main design procedure. Let $\{w_0, w_1, w_2, \dots, w_{2K-1}\}$ be the desired $2K$ weights of the data window. The spectral window can be written as

$$W(f) = \sum_{k=0}^{2K-1} w_k e^{-j2\pi f k T} \quad (19)$$

which can be expressed as a polynomial of $u = \cos \pi f T$:

$$W(f) = 2e^{-j(2K-1)\pi f T} u \prod_{k=1}^{K-1} (u^2 - \xi_k^2) \Big|_{u=\cos \pi f T} \quad (20)$$

where $\{\xi_k\}$ are the zeros of the polynomial. By controlling the locations of the zeros one can form a spectral window with a desired sidelobe structure. To suppress near-sidelobes the zeros $\{\xi_k\}$ can be chosen as follows:

$$\xi_k = \cos\left(\frac{\pi Z_k}{2K}\right) \quad k=1, 2, \dots, K-1 \quad (21)$$

where

$$Z_k = k \quad \text{for } k \geq k_0 \quad (22)$$

and

$$Z_{k-1} = Z_k - \Delta_k \quad \text{for } 1 \leq k \leq k_0 \quad (23)$$

with

$$\Delta_k = 1 - A \sin\left[\left(\frac{k_0 - k}{k_0 - 1}\right) \frac{\pi}{2}\right] \quad (24)$$

In (23) and (24), Δ_k is the increment of $\{Z_k\}$, k_0 is the number of the near-sidelobes to be suppressed, and A is a parameter to control the near-sidelobe level. In [7] a Tseng window is designed with $k_0=4$ and $A=0.7$, which yields a spectral window with near-sidelobes of -47 dB.

4. Numerical Examples:

We now consider a real time signal given by

$$\begin{aligned} x(t) = & V_1 e^{-\sigma_1 t} J_0(2\pi f_1 t) + V_2 e^{-\sigma_2 t} \cos(2\pi f_2 t) \\ & + V_3 e^{-\sigma_3 t} J_0(2\pi f_3 t) + V_4 e^{-\sigma_4 t} \cos(2\pi f_4 t) \end{aligned} \quad (25)$$

which contains two pairs of branch points:

V_1 at $-\sigma_1 \pm j2\pi f_1$ and V_3 at $-\sigma_3 \pm j2\pi f_3$ and two pairs of poles:

V_2 at $-\sigma_2 \pm j2\pi f_2$ and V_4 at $-\sigma_4 \pm j2\pi f_4$

The signal $x(t)$ is uniformly sampled at a sampling rate of 10240 Hz. A total of 128 samples are taken. To suppress picket-fence effect we added 384 zeros to the sampled data. A modified FFT is then applied to this 512 data points along a contour located at $\sigma = -\sigma_0$.

For the first example, we let the branch points $V_1=V_3=1.0$ (0 dB) at $f_1 = 1000$ Hz and $f_3 = 2000$ Hz, and the poles are $V_2=V_4=0.1$ (-20 dB) at $f_2 = 1500$ Hz and $f_4 = 2250$ Hz. Fig. 3 shows the amplitude spectra for the rectangular and the Tseng windows when the contour is along $\sigma = -100$. It illustrates that the Tseng window yields better resolution.

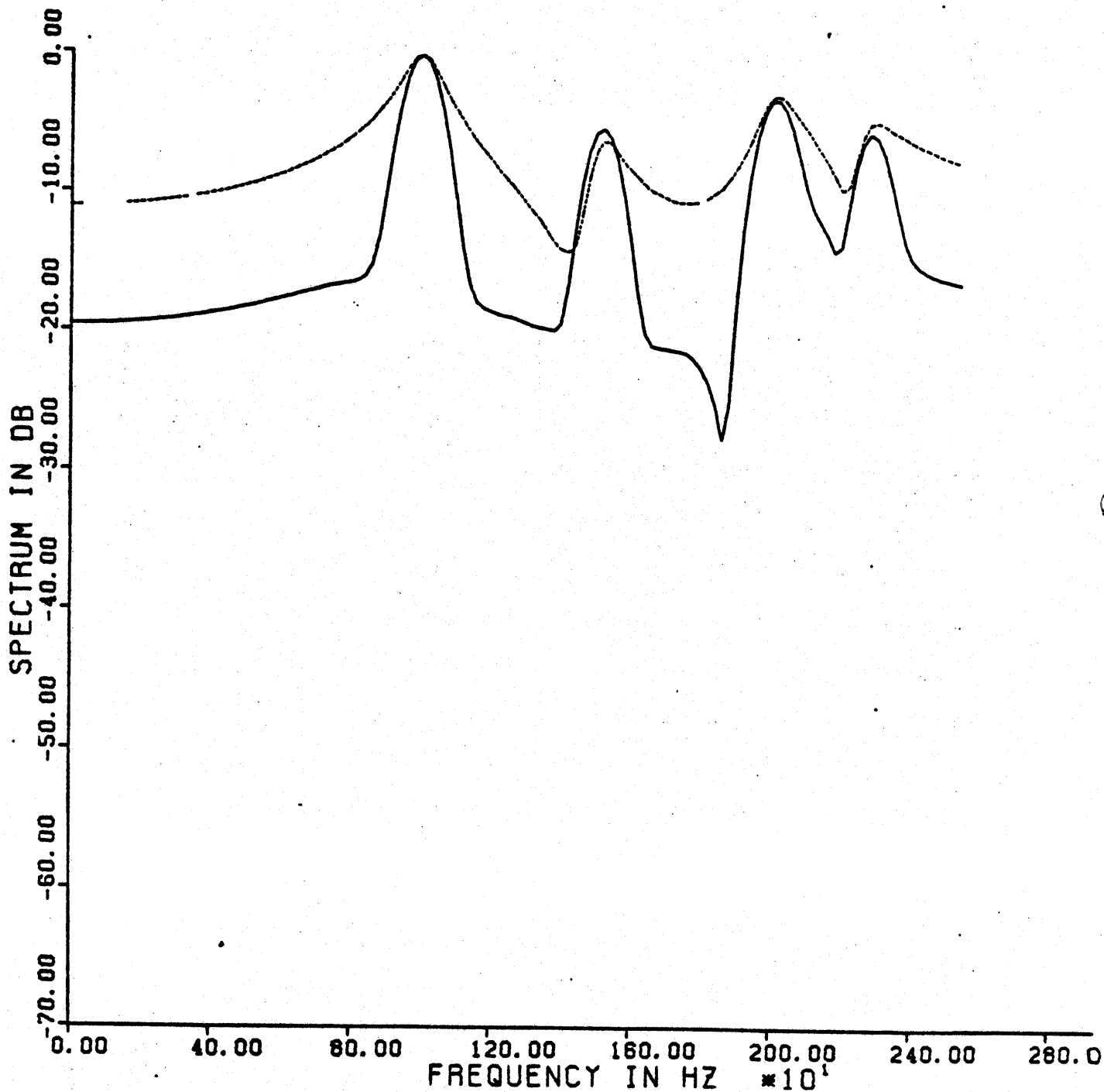


Fig. 3. Amplitude spectra for detecting branch points ($V_1=0$ dB, $f_1=1000$ Hz, $\sigma_1=-150$; $V_3=0$ dB, $f_3=2000$ Hz, $\sigma_3=-150$) and poles ($V_2=-20$ dB, $f_2=1500$ Hz, $\sigma_2=-150$; $V_4=-20$ dB, $f_4=2250$ Hz, $\sigma_4=-150$)² with Tseng window (solid) and rectangular window (dash); $\sigma_0=-100$.

Fig. 4 shows the phase spectra. Since the singularities are located at $\sigma=-150$ while the contour is on $\sigma=-100$, the phase variations at the singularities are less than 90° for the rectangular window while for the Tseng window, the phase variations are much steeper. The Tseng window also shows larger phase variations on the poles (about 170°) as compared to the branch points (about 130°). As the contour cuts across the singularities at $\sigma=-150$, the phase spectra of Fig. 5 show that there are smaller phase variations (about 110°) at the branch points than at the poles (about 190°) for the rectangular window, while the Tseng window results in higher phase variations.

For the next example, the branch points are assumed to be small: $V_1=V_3=0.1$ (-20 dB) while the poles have large amplitudes: $V_2=V_4=1.0$ (0 dB) but located at $\sigma_2=-200$ and $\sigma_4=-250$. Figure 6 shows the amplitude spectra along the $j\omega$ -axis ($\sigma=0$). It shows that both windows failed to detect the small branch points. Now, as the contour cuts at $\sigma=-150$, the Tseng window shows the ability to detect the branch point at 1000 Hz while the rectangular window cannot detect any branch points. Figure 8 illustrates that both windows indicate small phase variation at the branch points but much larger variations at the poles. Figure 9 presents the phase increments as functions of the frequency. It is seen that, even though the amplitude spectra using both windows failed to detect the branch point at $f_3=2000$ Hz, the phase increment spectra indicate a singularity at $f_3=2000$ Hz. Notice also that the phase increment patterns at the two branch points are quite different from those at the poles. This is due to the fact that the contour cut across

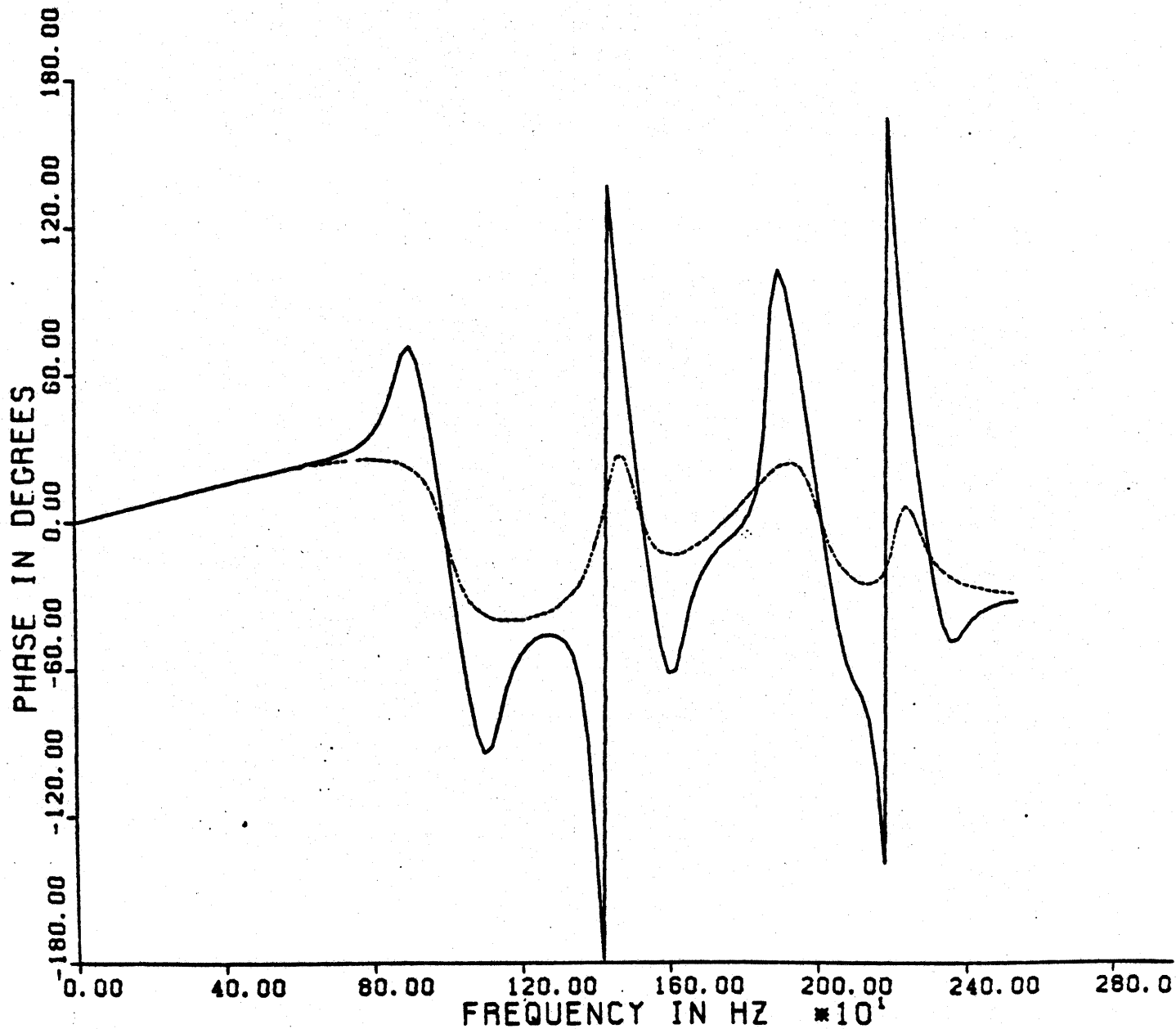


Fig. 4. Phase spectra for detecting branch points ($V_1=0$ dB, $f_1=1000$ Hz, $\sigma_1=-150$; $V_3=0$ dB, $f_3=2000$ Hz, $\sigma_3=-150$) and poles ($V_2=-20$ dB, $f_2=1500$ Hz, $\sigma_2=-150$; $V_4=-20$ dB, $f_4=2250$ Hz, $\sigma_4=-150$) with Tseng window (solid) and rectangular window (dash); $\sigma_0=-100$.

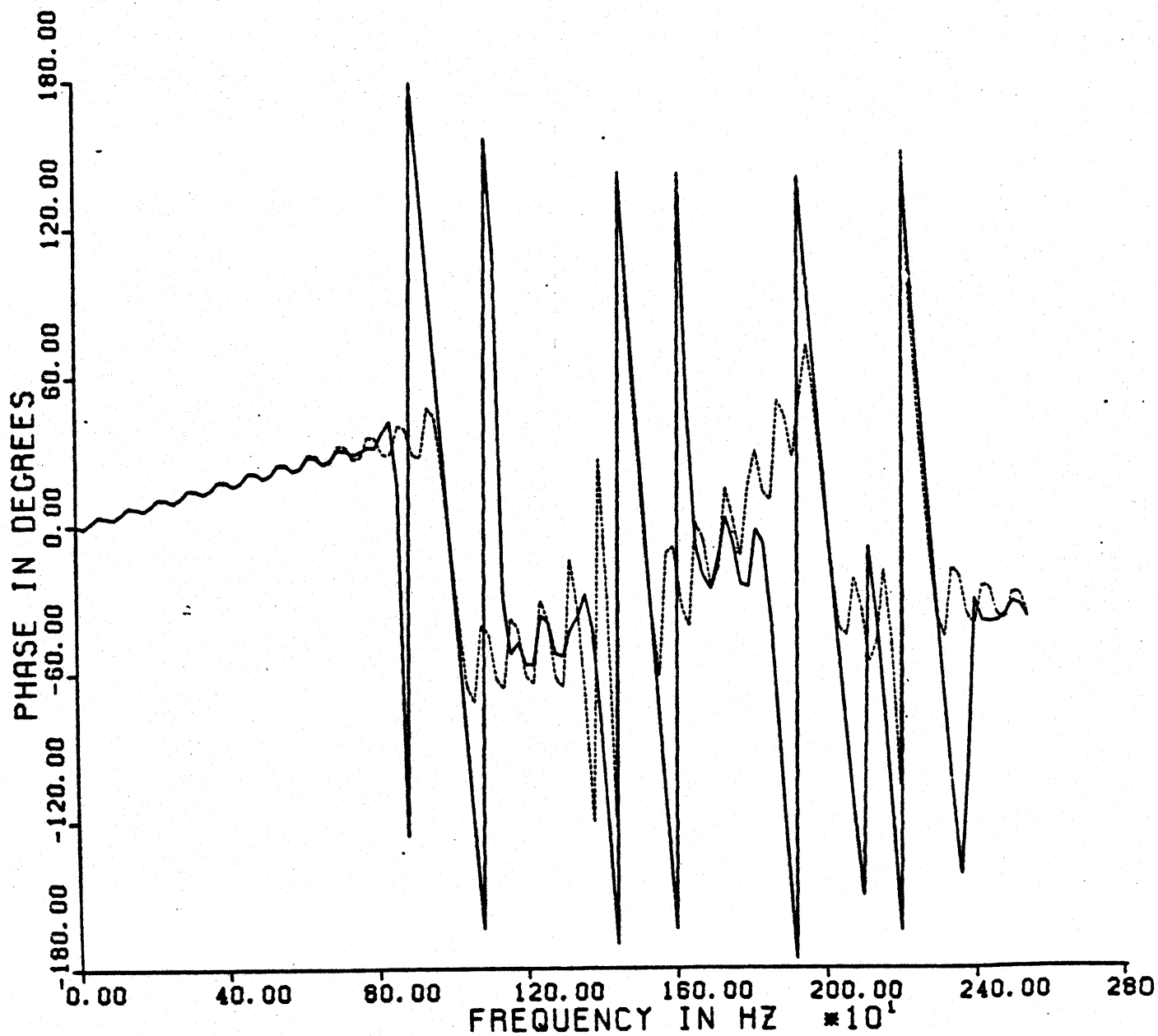


Fig. 5. Phase spectra for detecting branch points ($V_1=0$ dB, $f_1=1000$ Hz, $\sigma_1=-150$; $V_3=0$ dB, $f_3=2000$ Hz, $\sigma_3=-150$); and poles ($V_2=-20$ dB, $f_2=1500$ Hz, $\sigma_2=-150$; $V_4=-20$ dB, $f_4=2250$ Hz, $\sigma_4=-150$) with Tseng window (solid) and rectangular window (dash); $\sigma_0=-150$.

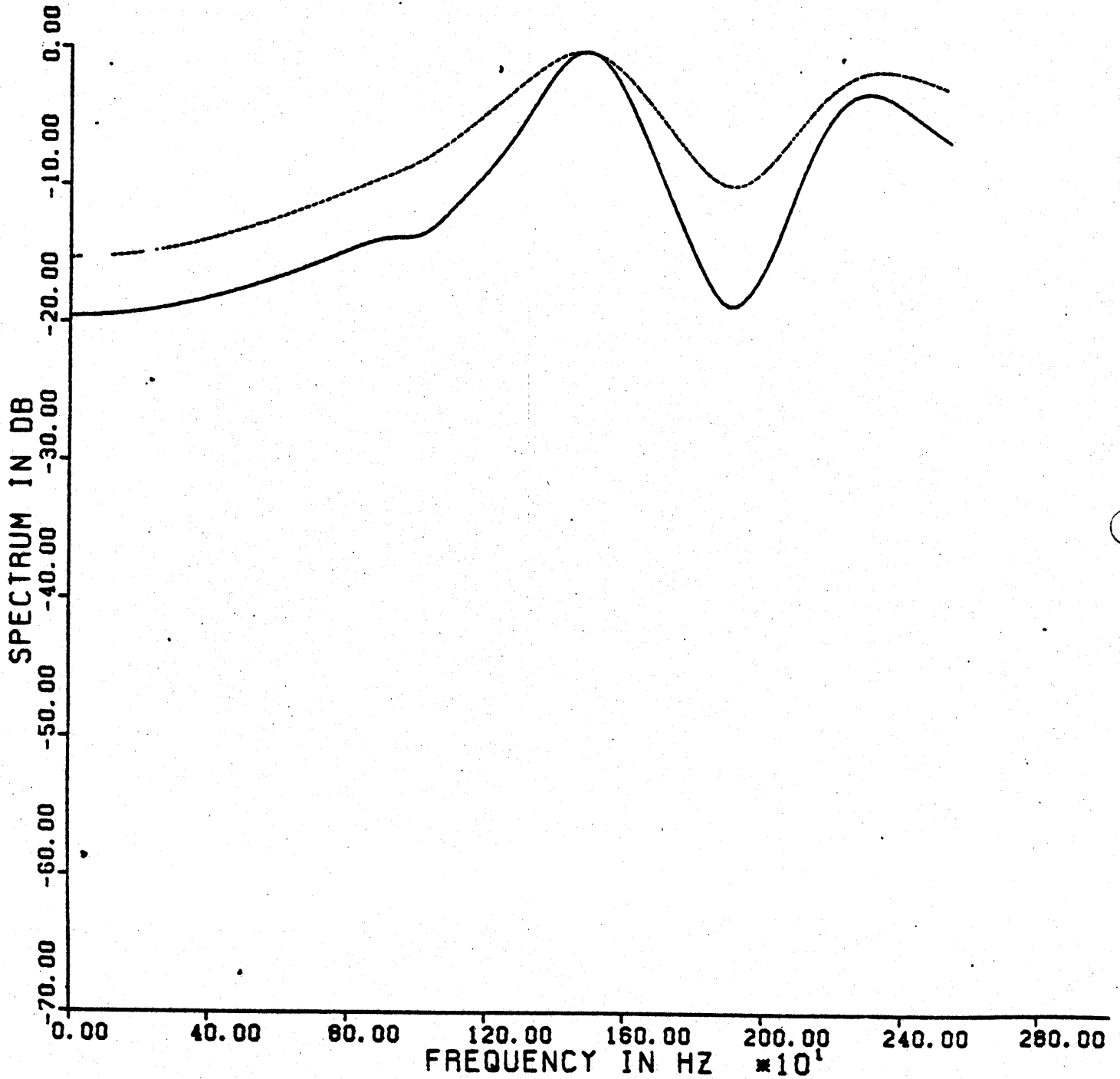


Fig. 6. Amplitude spectra for detecting branch points ($V_1 = -20$ dB, $f_1 = 1000$ Hz, $\sigma_1 = -150$; $V_3 = -20$ dB, $f_3 = 2000$ Hz, $\sigma_3 = -150$); and poles ($V_2 = 0$ dB, $f_2 = 1500$ Hz, $\sigma_2 = -200$; $V_4 = 0$ dB, $f_4 = 2250$ Hz, $\sigma_4 = -250$)² with Tseing window (solid) and rectangular window (dash); $\sigma_0 = 0$.

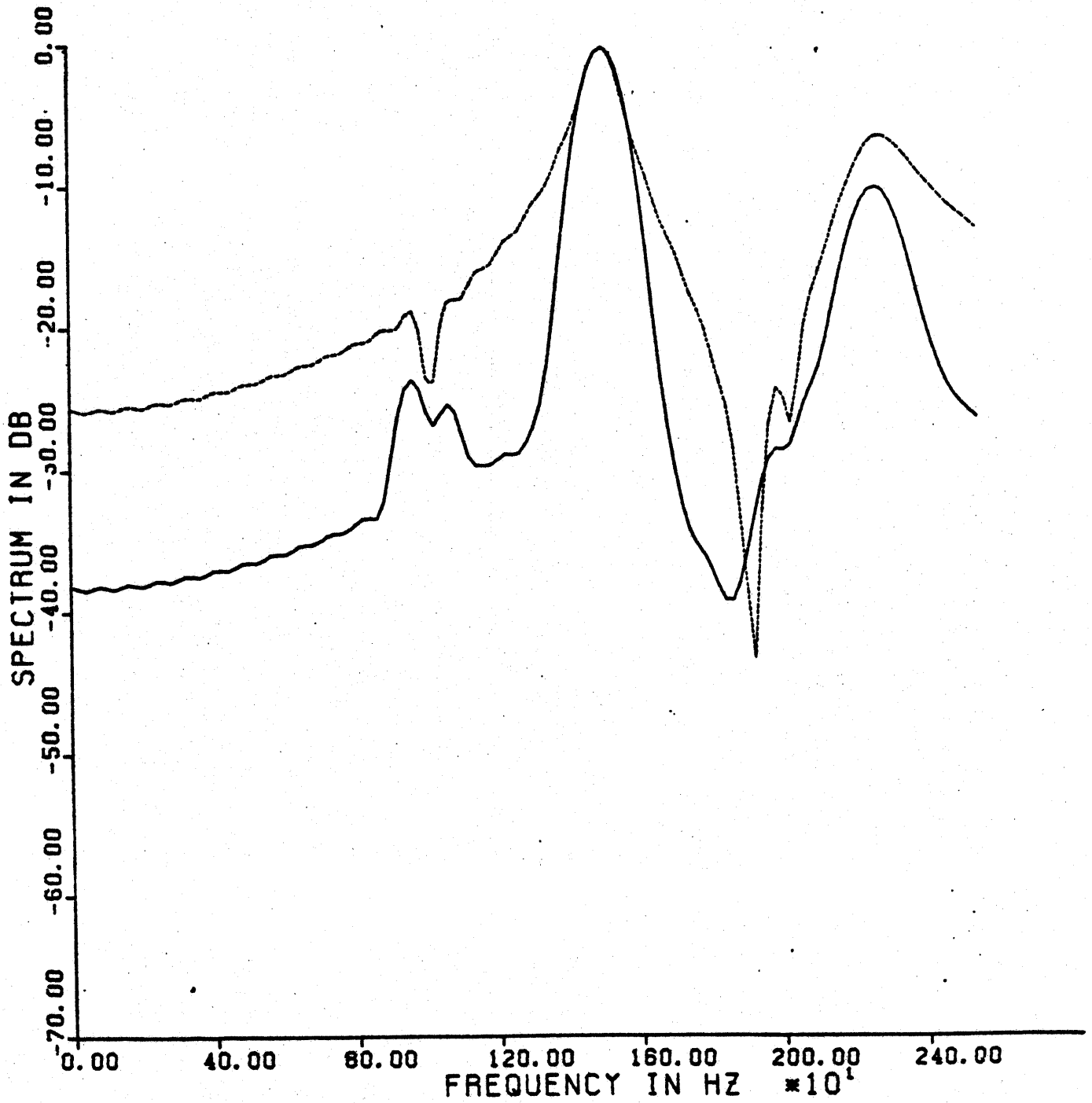


Fig. 7. Amplitude spectra for detecting branch points ($V_1 = -20$ dB, $f_1 = 1000$ Hz, $\sigma_1 = -150$; $V_3 = -20$ dB, $f_3 = 2000$ Hz, $\sigma_3 = -150$); and poles ($V_2 = 0$ dB, $f_2 = 1500$ Hz, $\sigma_2 = -200$; $V_4 = 0$ dB, $f_4 = 2250$ Hz, $\sigma_4 = -250$), with Tseng window (solid) and rectangular window (dash); $\sigma_0 = -150$. 15

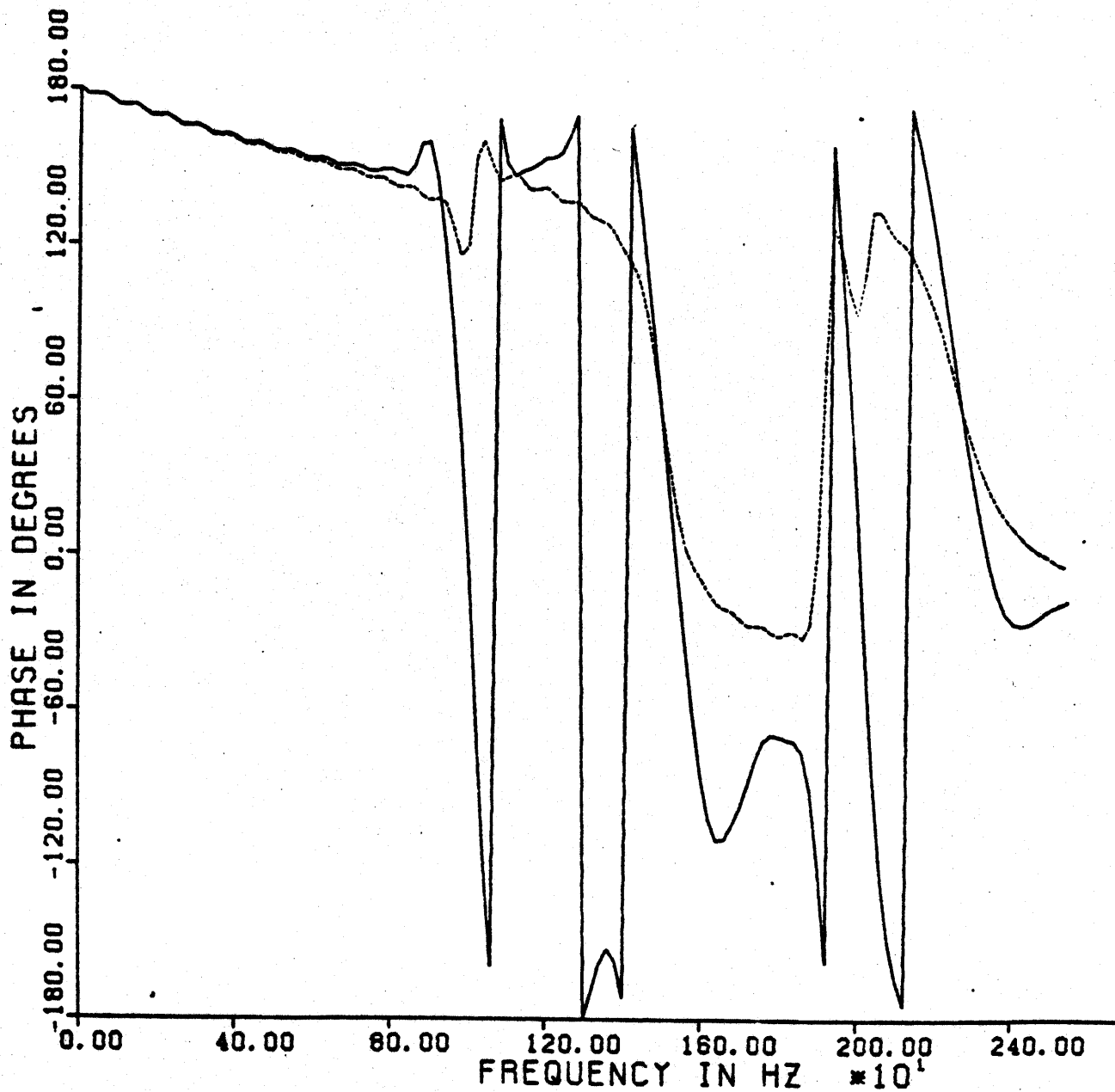


Fig. 8. Phase spectra for detecting branch points ($V_1 = -20$ dB, $f_1 = 1000$ Hz, $\sigma_1 = -150$; $V_2 = -20$ dB, $f_2 = 2000$ Hz, $\sigma_2 = -150$); and poles ($V_3 = 0$ dB, $f_3 = 1500$ Hz, $\sigma_3 = -200$; $V_4 = 0$ dB, $f_4 = 2250$ Hz, $\sigma_4 = -250$)² with Tseing window (solid) and rectangular window (dash); $\sigma_0 = -150$.

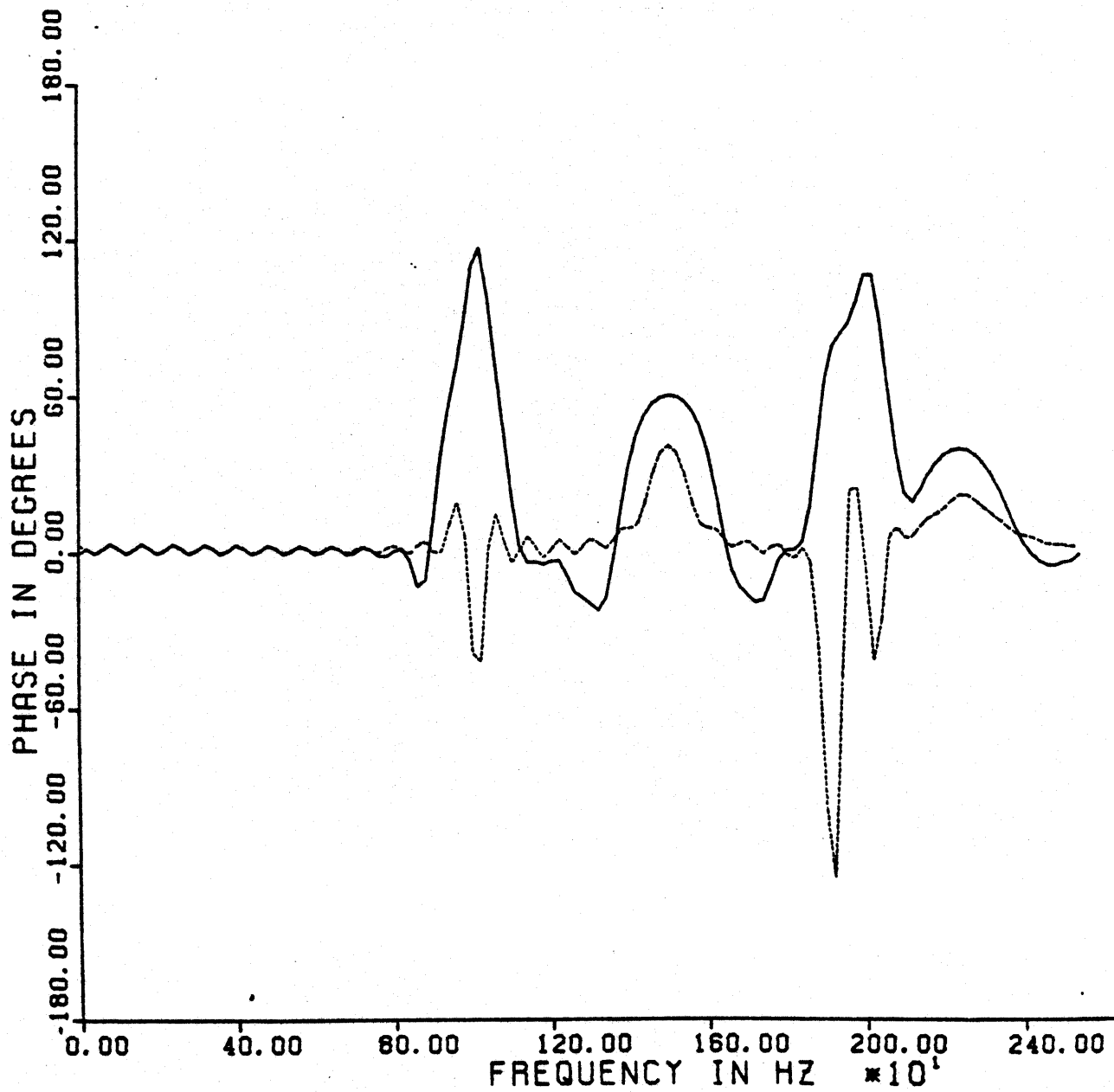


Fig. 9. Phase increment spectra for detecting branch points, ($V_1 = -20$ dB, $f_1 = 1000$ Hz, $\sigma_1 = -150$; $V_3 = -20$ dB, $f_3 = 2000$ Hz, $\sigma_3 = -150$); and poles ($V_2 = 0$ dB, $f_2 = 1500$ Hz, $\sigma_2 = -200$; $V_4 = 0$ dB, $f_4 = 2250$ Hz, $\sigma_4 = -250$) with Tseng window (solid) and rectangular window (dash); $\sigma_0 = -150$.

the branch points but stay away from the poles. There seems to be a correlation between the sharpness of the phase increment pattern and the closeness of the singularity to the contour.

5. Conclusions:

A new technique of detecting a branch point in transients is presented in this paper. The new technique employs the phase information in the modified FFT to distinguish a branch point from a pole. Several examples demonstrate the effectiveness of the technique. It also shows the importance of choosing proper contours in evaluating the modified FFT. And by the use of windowing it is possible to detect a small branch point under the influence of a nearby strong pole.

References

- 1 C.E.Baum, "Emerging Technology for Transient and Broad-band Analysis and Synthesis of Antennas and Scatterers," Proc. IEEE, Vol. 64, No. 11, p. 1598, Nov. 1976, also Interaction Note 300, Nov 76.
- 2 O.M. Bucci and G. Franceschetti, "Input Admittance and Transient Response of Spheroidal Antennas in Dispersive Media," IEEE Trans. Antennas & Propagation, Vol. AP-22, p. 256, July 1974.
- 3 G. Franceschetti, "A Canonical Problem in Transient Radiation - The Spherical Antenna" IEEE Trans. Antennas & Prop. Vol. AP-26, No. 4, p. 551, July 1978.
- 4 N. Nahman and D. Holt, "Transient Analysis of Coaxial Cables Using the Skin Effect Approximation A+B s ", IEEE Trans. Circuit Theory, Vol. CT-19, No. 5, p. 443, Sept. 1972.
- 5 D. Holt and N. Nahman, "Coaxial-Line Pulse-Response Error Due to a Planar Skin-Effect Approximation," IEEE Trans. Instrumentation and Measurement, Vol. IM-21, No. 4, p. 515, Nov. 1972.
- 6 C.T. Tai, "Transients on Lossless Terminated Transmission Lines," IEEE Trans. Antennas Propagation Vol. AP-26, No. 4, p. 556, July 1978, also Interaction Note 312, 8 Jun 77.
- 7 F.I.Tseng and T.K.Sarkar, "Enhancement of Poles in Spectral Analysis," IEEE Trans. Geoscience and Remote Sensing (to be published, April 1982), also Mathematics Note 72, November 81.
- 8 F.I. Tseng, T.K. Sarkar and D.D. Weiner, "A Novel Window for Harmonic Analysis," IEEE Trans. on Acoustics, Speech and Signal Processing, Vol. ASSP-29, No. 2, April 1981.